LAWRENCE
LIVERMORE
NATIONAL
LABORATORY

LLNL-JRNL-409789

Turbulence Considerations for Comparing Ecosystem Exchange over Old-Growth and Clear-Cut Stands For Limited Fetch and Complex Canopy Flow Conditions

S. Wharton, M. Schroeder, K. T. Paw U, M. Falk, K. Bible

January 12, 2009

Agricultural and Forest Meteorology

Disclaimer

Turbulence Considerations for Comparing Ecosystem Exchange over Old-Growth and Clear-Cut Stands For Limited Fetch and Complex Canopy Flow Conditions

Sonia Wharton[1*], Matt Schroeder[2], Kyaw Tha Paw U[1], Matthias Falk[3] and Ken Bible[2]

[1]Atmospheric Science, University of California, Davis, California; [2]College of Forest Resources, University of Washington, Seattle; [3]CSTARS, University of California, Davis, California

*Corresponding author now at: Atmospheric, Earth and Energy Division, Lawrence Livermore National Lab, P.O. Box 808, L-103, Livermore, CA 94551, USA, Tel. ++1-925-422-9295, email: wharton4@llnl.gov

LLNL-JRNL-409789

Keywords: *old-growth, clear-cut, Douglas-fir, ecosystem exchange, fetch, footprint modeling, turbulence statistics*

Abstract

Carbon dioxide, water vapor and energy fluxes were measured using eddy covariance (EC) methodology over three adjacent forests in southern Washington State to identify stand-level age-effects on ecosystem exchange. The sites represent Douglas-fir forest ecosystems at two contrasting successional stages: old-growth (OG) and early seral (ES). Here we present eddy flux and meteorological data from two early seral stands and the Wind River AmeriFlux old-growth forest during the growing season (March-October) in 2006 and 2007. We show an alternative approach to the usual friction velocity (u_*) method for determining periods of adequate atmospheric boundary layer (ABL) mixing based on the ratio of mean horizontal ($\overline{u}$) and vertical ($\overline{w}$) wind flow to a modified turbulent kinetic energy scale (u_{TKE}). This new parameter in addition to footprint modeling showed that daytime CO_2 fluxes (F_{NEE}) in small clear-cuts (< 10 hectares) can be measured accurately with EC if micrometeorological conditions are carefully evaluated.

Peak midday CO_2 fluxes (F_{NEE} = - 14.0 to -12.3 μmol m^{-2} s^{-1}) at OG were measured in April in both 2006 and 2007 before bud break when air and soil temperatures and vapor pressure deficit were relatively low, and soil moisture and light levels were favorable for photosynthesis. At the early seral stands, peak midday CO_2 fluxes (F_{NEE} = - 11.0 to -8.7 μmol m^{-2} s^{-1}) were measured in June and July while spring-time CO_2 fluxes were much smaller (F_{NEE} = - 3.8 to -3.6 μmol m^{-2} s^{-1}). Overall, we measured lower evapotranspiration (OG = 230 mm; ES = 297 mm) higher midday F_{NEE} (OG F_{NEE} = -9.0 μmol m^{-2} s^{-1}; ES F_{NEE} = -7.3 μmol m^{-2} s^{-1}) and higher Bowen ratios (OG β = 2.0. ES β = 1.2) at the old-growth forest than at the ES sites during the summer months (May-August). Eddy covariance studies such as ours add critical land-atmosphere exchange data for an abundant, but rarely studied Douglas-fir age class.

1. Introduction

The Pacific Northwest region of the U.S. is one of the most productive forested areas in the world and its future role in the terrestrial carbon cycle will be dependent on how silviculture practices alter the age structure of these forests (Song and Woodcock 2002). Over the past 50 years, staggered-set clear-cutting on local Federal lands has created a fragmented landscape of different age Douglas-fir forests ranging from early seral (ES) (0-15 years), young (less than 80 years old), intermediate (80 to 200 years), mature (200 to 400 years), to old-growth (OG) (approximately greater than 400 years old). While early seral stands can compromise up to 40% of total forest coverage in the Western Cascade Mountains (Cohen et al. 1996) and are an essential component of any regional assessment of CO_2 fluxes, ecosystem exchange within this youngest age class has not been thoroughly studied with eddy covariance (EC).

Ecosystem responses to seasonal climate (e.g., summer drought), timing of extreme weather events (e.g., summer rain pulses) and phenological changes (e.g., bud break) likely vary with stand age and affect biosphere-atmosphere exchange. Yet, our understanding of stand-level age-effects remains limited for several reasons. One difficultly that often restricts chronosequence flux studies is different successional stages may have vastly different species compositions making it hard to compare mature and young forest sites for age-effects. All of our study sites at Wind River are dominated or co-dominated by Douglas-fir, an extremely long-lived (up to ~700 years) pioneering species. Secondly, the placement of study sites must be carefully considered to reduce regional or terrain-induced weather differences from misinterpreting stand-level comparisons. This means that the forests of interest may need to be within a couple of kilometers of each other in a complex terrain environment. And lastly, since early seral stands are often the result of a size-restricted harvest on Federal lands, they are

limited by the availability of fetch. This creates a unique set of micrometeorological concerns for the eddy covariance technique which will be discussed next.

A desirable fetch to instrument height ratio in micrometeorological applications is dependent on atmospheric boundary layer (ABL) stability and surface-canopy roughness but has generally been accepted at ~ 40:1 (e.g., Kruijt 1994, Schmid 1994, Irvine et al. 1997). Fetch requirements in small, individual forest stands (e.g., clear-cuts) within a heterogeneous vegetative area are less certain and may be more site specific. One study by van Breugel et al. (1999) found that a fetch:instrument height ratio of 36:1 ensured that EC instruments were measuring turbulent fluxes within the equilibrium layer (part of the atmosphere where the local stress is largely in equilibrium with the underlying vegetative surface) under most atmospheric conditions over a patchy Netherlands forest landscape. A similar, but broader fetch:instrument height range was estimated at 25 to 50:1 by Kolari et al. (2004) who looked at turbulent fluxes over a 7 hectare, 12-year old clear-cut in Southern Finland. Equilibrium layer depth in addition to being sensitive to site-specific canopy roughness also varies dramatically during the course of a day. The ABL tends towards stable conditions at night and moderately stable-to-convective conditions during the day depending on the production and dissipation of buoyancy-driven turbulence and production of shear-generated turbulence. Atmospheric mixing near the surface is further complicated by variable topography which creates complex wind flows including strong, along-valley-axis flows (wind direction shifts) and gravity-driven, mountain-valley flows that are particularly strong at night.

Prior chronosequence flux studies in very young (re-established after a clear-cut disturbance) and mature conifer forests have not shown universal results in regards to stand-age effects on ecosystem exchange. Most of the site variability has occurred in the growing season

energy and water vapor fluxes, while CO_2 exchange tends to have greater age-specific trends. Some research suggests that evapotranspiration (E_T) totals in early seral and mature forests are nearly equal (Amiro et al. 2006) while other studies have found significant age-related differences (Anthoni et al. 2002). Nearly all age-effect studies have shown that net carbon uptake is greater in mature conifer stands than in the 0-20 year age class (e.g., Anthoni et al. 2002, Irvine et al. 2002, Law et al. 2003, Thomas and Winner 2002, Amiro et al. 2006, Humphreys et al. 2006).

At Wind River, four Douglas fir age classes have been studied for age-effects on CO_2 or H_2O exchange: early seral (this study, Bauerle et al. 1999, Thomas and Winner 2002), 20-year old (Chen et al. 2002, 2004, Phillips et al. 2002, McDowell et al. 2005), 40-year old (Chen et al. 2002, 2004, Phillips et al. 2002) and old-growth (this study, Bauerle et al. 1999, Chen et al. 2002, 2004, Phillips et al. 2002, Thomas and Winner 2002, Paw U et al. 2004, Unsworth et al. 2004, Winner et al. 2004, Falk et al. 2005, 2008). Even across the Wind River chronosequence the studies have not shown similar age-related results. For example, Chen et al. (2004) and Thomas and Winner (2002) report higher photosynthetic rates in the old-growth trees than at the youngest stands while McDowell et al. (2005) and Bauerle et al. (1999) found no significant age-related differences.

Our study represents the longest, continuous record of flux exchange at Wind River for the early seral age class. Presented are data from two early seral stands of nearly identical age and species composition. Our goals are to (1) determine whether fluxes can be accurately measured in typical Douglas-fir early seral stands, and (2) identify seasonal or monthly flux differences between the different-age stands. An in-depth ecophysiological response to age-effects analysis will be presented in a future paper.

2. Site Description and Instrumentation

2.1 Overview

Despite the surrounding complex terrain of the Western Cascade Mountains, all three forest sites are located in a relatively flat valley (slope is 3.5%) in southern Washington State. The predominant wind direction is from the west although valley flow (northwest-southeast) wind shifts are also common. The climate at Wind River is dominated by two distinct seasons: a cool, wet winter and a warm, dry summer. Very little rain (<10% of 2233 mm annual total) typically falls in July and August and consistent precipitation usually does not return to the area until the end of October. This study uses daily precipitation (P) data collected 5 km north of Wind River at the NOAA Carson Fish Hatchery Meteorological Station (45º31'12" N, 121º34'48" W; 345.6 m a.s.l.) and acquired from the National Climatic Data Center (http://cdo.ncdc.noaa.gov/CDO/cdo). EC and micrometeorological data were measured continuously at the old-growth forest from January 2006 (OG06) through December 2007 (OG07) although winter data (November – February) are not presented here. Data were collected at Early Seral North (ESN06) during the 2006 growing season and at Early Seral South (ESS07) during the 2007 growing season. Growing season is defined here as March through October; drought season as July through October. Detailed data availability periods and gap-filled data percentages are listed in Table 1.

2.2 Old-growth forest

The Wind River Canopy Crane (45°49'13.76" N, 121°57'06.88" W; 371 m above sea level) is located in a 500-hectare old-growth, coniferous forest in the T.T. Munger Research Natural Area, a protected section of the Gifford Pinchot National Forest (figure 1). The site has

been unmanaged for centuries since originating from a natural fire disturbance. Shaw et al. (2004) provide a detailed site description for the Wind River old-growth forest. In brief, the two dominant tree species are Douglas-fir (*Pseudotsuga menziesii* (Mirbel) Franco) and western hemlock (*Tsuga heterophylla* (Raf.) Sarg.). Trees within the stand range in age from 0 to approximately 500 years old and reach maximum heights of 65 meters. Leaf area index (LAI) is between 8.2 - 9.2 m^2 m^{-2} (Parker et al. 2004) and does not change significantly from year to year or season to season. Despite a co-dominance of western hemlock, Douglas-fir likely exert significant control over carbon uptake in the stand since their crowns are located in the highest light environment of all canopy species (Thomas and Winner 2000). The soils are classified as medial, mesic, Entic Vitrands 2-3 meters deep. Most tree roots are found within the first 0.5 m although roots of Douglas-fir can extend depths of 1 to 2 meters. These soils are homogeneous, rock-free and have a low bulk density and high organic matter content. The water table generally ranges from 0.4 m in the winter rainy season to 2 m in late summer (Shaw et al. 2004).

We provide a short description of the eddy covariance set-up here while a more detailed description of the methodology can be found in Paw U et al. (2004), Falk (2005) and Falk et al. (2008). The EC system consisted of a sonic anemometer (Solent HS, Gill Instruments, Lymington, England, UK) and a closed-path infrared gas analyzer (IRGA) (LI-7000, LiCor, Lincoln, Nebraska, USA) which measured the wind velocity vectors and sonic temperature, and concentrations (mixing ratios) of H_2O and CO_2, respectively, at 10 Hz. The IRGA and sonic anemometer were mounted at the end of a 5 meter boom at a height of 67 meters on the crane tower so that the anemometer faced west towards the maximum area of homogeneous vegetation. Footprint modeling (following Wilson and Swaters 1991) was done by Paw U et al. (2004) and

Falk (2005). Their results showed that fetch was good (200 m or less) in all directions under very unstable conditions, but problematic (1-10 km) under stable conditions due to fragmented age classes beyond the old-growth stand.

Air temperature and relative humidity (sheltered HMP-35C, Vaisala, Inc., Oy, Finland) and photosynthetically active radiation (PAR) (190-SB, LiCor) were measured at heights of 2 m (below canopy) and 70 m (above canopy) along the canopy crane tower. Vapor pressure deficit (VPD) was calculated from air temperature and relative humidity measurements. Volumetric soil water content was measured nearby at an integrated depth of 0-30 cm in 2006 with a time-domain reflectometry (TDR) system (TDR100, Campbell Scientific). In 2007, soil water content was measured with four Sentek soil moisture probes at incremental depths from 20 to 200 cm (Sentek EnviroSMART, Sentek Sensor Technologies, Stepney, Australia). The ground heat flux was measured with a HFT-3.1 soil heat flux plate buried 7.5 cm below the surface. The meteorological measurements were collected as 30-minute averages.

2.3 Early seral north

The early seral north (ESN06, measured in 2006) flux tower (45^{o}49'37.2" N, 121^{o}57'39.6" W; 361 m a.s.l.) was located in a 7 ha. clear-cut on the southeastern foot of Trout Creek Hill and was 1.25 km northwest of the Wind River Canopy Crane (figure 1). Topographic slope is from west to east and is less than 10 percent. This is a third generation Douglas-fir forest: the original old-growth trees were logged in 1920 and a clear-cut harvest was done in 1994 on 80-year old Douglas-fir. The harvested stand is surrounded by 40 meter tall, 80-year old trees. In 1997, five plots were planted with Douglas-fir (*Pseudotsuga menziesii*) and red alder (*Alnus rubra*) samplings as part of a Hardwood Silviculture Cooperative Type 3 project. Each was seeded with

741 tree ha^{-1} in various species proportions and no fertilization treatments were applied. In September 2005 we erected a 6 meter tall flux tower in the 100% Douglas-fir planted section. At that time standing biomass measurements were taken (n=45): mean tree height was 4.4 m, height range was 1.2 to 5.3 m, and mean diameter at breast height (d.b.h) was 5.7 cm. The five planting blocks covered roughly half of the 7 hectare area; the remainder was dominated by naturally seeded Douglas-fir. Western hemlock (*Tsuga heterophylla*) and western white pine (*Pinus monticola*) seedlings were also present in insignificant amounts. Dominant ground cover species included salal (*Gualtheria shallon*), Oregon grape (*Berberis nervosa*), bracken fern (*Pteridium aquilinum*), sword fern (*Polystichum munitum*) and blackberry (*Rubus ursinus*).

EC estimates of vertical H_2O and CO_2 fluxes were made using a CSAT-3 sonic anemometer (Campbell Scientific) and an open-path fast response LI-7500 IRGA which measured the wind velocity vectors, air temperature, and densities of CO_2 and H_2O vapor above the canopy. The sonic anemometer was mounted facing west-southwest and pointed in the direction of greatest homogenous fetch (200 m of even-aged Douglas-fir). Both the LI-7500 and CSAT-3 were mounted at 5.5 m a.g.l., 1.1 m above the canopy, on a boom extending from a 6 m tall triangular-frame steel tower. The EC data were measured at 10 Hz and 30-minute averages were archived in the field using a CR1000 data logger (Campbell Scientific). Meteorological data included half-hour measurements of air temperature/relative humidity (sheltered HMP-35C, Vaisala, Inc.), net radiation (Q7.1, Radiation and Energy Systems, Seattle, Washington, USA), soil temperature (5, 10 and 15 cm) (CS106B, Campbell Scientific) and soil moisture (2 replicates of 0-30 and 30-60 cm integrated depths) (Time-domain reflectometry (TDR) system, TDR100, Campbell Scientific).

2.4 Early seral south

The early seral south (ESS07, measured in 2007) flux tower (45°48'47.4" N, 121°57'32.9" W; 371 m a.s.l.) was located in a 10 hectare abandoned clear-cut (1985), 910 m southwest of the canopy crane (figure 1) and was naturally established with Douglas-fir from surrounding cone crops. Tree measurements were taken three times at four month intervals in 2007. Average tree height (n=95) was 3.3 ± 0.8 m in April, 3.9 ± 0.9 m in July and 4.0 ± 1.0 m in October. D.b.h. was additionally measured in July (4.6 ± 1.6 cm) and October (4.7 ± 1.4 cm). Estimated tree density was 1063 trees per hectare (8 sampled plots of 100 m^2 each). Above-ground biomass (stem wood + stem bark + live branch + total foliage) was estimated at 14.5 Mg C ha^{-1} using allometric equations derived from regional Douglas-fir data (Grier and Logan 1977). The average Douglas-fir tree was 9 to 14 years of age in July 2007 (tree coring, n=10). Other tree species included western white pine, red alder and planted Pacific silver fir (*Abies amabilis*) and Pacific yew (*Taxus brevifolia*) seedlings in insignificant amounts. Bracken fern was the dominant ground species. Grass species and scotch broom (*Cytisus scoparius*) were also common in the more open areas. The EC system was identical to the setup used at ESN except that the sonic anemometer was mounted facing south and the instruments were placed at a height of 5 m, 1.4 m above the canopy. The meteorological instrumentation was also identical to ESN, and in addition we added up- and down-facing PAR sensors (190-SB, LiCor) and 2 TDR soil moisture probes at 60-90 cm depth. All early seral instrumentation were powered using a 110 W solar panel and bank of batteries. Soil samples (3 replicates at 2 measurement depths) were dug up at ESN06 and ESS07 and brought to the ANR Analytical Laboratory at UC Davis for analysis in September 2007.

3. Materials and Methods

3.1 Flux calculations and corrections

Old-growth stand

Fluxes of carbon dioxide (F_c, μmol CO_2 m^{-2} s^{-1}), water vapor (F_{H2O}, mmol H_2O m^{-2} s^{-1}), sensible heat (H, W m^{-2}) and latent heat (λE, W m^{-2}) were computed from 10 Hz eddy covariance data using an in-house FORTRAN90 code with a time averaging period of 30 minutes and a horizontal coordinate rotation (mean cross-wind velocities were forced to zero). The rate of change in CO_2 concentration (storage flux, S_c, μmol CO_2 m^{-2} s^{-1}) within the canopy volume was estimated on a half-hourly basis using time changes in the mean CO_2 mixing ratio measured at the top of the canopy (Falk et al. 2008). To account for CO_2 stored within the canopy and below the detection height of the instruments, S_c was added to F_c to estimate net ecosystem exchange of carbon (F_{NEE}, μmol CO_2 m^{-2} s^{-1}) on a half-hourly basis. F_{NEE} and λE were further screened for incomplete half-hours, general instrument failure (e.g., pressure problems in the closed-path EC system), non-preferred wind directions (45° to 180°), major rain or snow events, or significant outliers (above or below the 95th confidence intervals). For complete details on old-growth flux post-processing see Paw U et al. (2004), Falk (2005) and Falk et al. (2008).

Early seral stands

At the two early seral stands F_c, F_{H2O}, H, and λE were calculated in real-time from 10 Hz covariance data using the CR1000 eddy covariance program (Campbell Scientific). The flux program used a 30-minute averaging period and included WPL80 (Webb et al. 1980) density corrections to eliminate air density fluctuation effects on CO_2 and H_2O fluxes. During post-processing all scalar and energy fluxes were re-calculated after the mean cross-wind (following

1 the natural wind coordinate system) and mean vertical wind velocities were forced to zero.
2 Calculated sonic anemometer tilt was 2.5° at ESN06 and 4° at ESS07. Prior to coordinate
3 rotation, average $\overline{w}$ was -0.02 m s^{-1} at ESN06 and -0.05 m s^{-1} at ESS07. The rate of change of
4 CO_2 concentration (S_c) within the canopy was estimated using the half-hourly changes in the
5 CO_2 mixing ratio measured at the top of the canopy and was added to F_c to estimate F_{NEE}.
6
7 *3.2 Data screening criteria at ESN and ESS*
8 The early seral flux data necessitated a different screening protocol than the old-growth
9 data for various reasons. First, continuous raw data (10 Hz) were not archived at the ES stands
10 which meant that some of the standard EC corrections could not be applied to the time series
11 (e.g., spectral corrections for frequency loss, optimization of time lag between w and CO_2 to
12 correct for IRGA and CSAT-3 sensor separation). Secondly, fetch availability and turbulence-
13 induced edge effects (from an abrupt rough-to-smooth canopy roughness transition) were a much
14 higher concern at the early seral stands and warranted the creation of data criteria 5 and 6 as
15 described below.
16 Half-hour F_{NEE}, F_{H2O} and energy fluxes were excluded from the time series if one or more
17 of the following criteria were met: (1) instrument malfunction or incomplete half-hour, (2)
18 "tower shadowing" or flow distortion around the CSAT-3, (3) heavy precipitation, (4) spike filter
19 = 1 (F_c only), (5) ratio of mean vertical or horizontal wind flow to turbulent velocity scale was
20 greater than the critical threshold, (6) insufficient fetch or (7) half-hourly variance was greater
21 than the 95^{th} and less than the 5^{th} confidence intervals. We used a spike filter methodology in
22 criterion (4) to detect significant half-hour CO_2 anomalies or outliers in the time series as
23 described in Papale et al. (2006). The spike filter algorithm is based on a double-differenced

time series and uses the median of absolute deviation about the mean (Sachs 1996) to detect unusually large deviations or "spikes" in the CO_2 flux record. Each 30-minute F_c was flagged if the spike filter equaled one and was replaced with a gap-filled value. The spike filter methodology removed 5% of available F_c data at ESN06 and 7% at ESS07.

Criterion (5) was used to identify half-hour fluxes measured during conditions when transport by mean flow could no longer be neglected compared to turbulent flow in the wind field. We reasoned that during these times the EC technique was not accurately measuring ecosystem exchange because a strong advective component reduced the fraction of exchange represented by the vertical turbulent exchange. This concern is illustrated by studying the Reynolds-averaged mass balance equation for biosphere-atmosphere exchange of CO_2:

$$\frac{\partial \overline{\rho_c}}{\partial t} + \frac{\partial (\overline{u_i}\,\overline{\rho_c})}{\partial x_i} + \frac{\partial (\overline{u'_i\,\rho'_c})}{\partial x_i} = \overline{S_c} \qquad (1)$$

Eqn. 1 shows that the CO_2 source or sink magnitude (net ecosystem exchange when integrated over the height of the canopy), $\overline{S}_c$, equals the sum of three terms: the rate of change in CO_2 storage (first term on LHS, estimated from measurement data in our study), the horizontal and vertical advective fluxes (second term, not measured or directly estimated in our study) and the eddy covariance fluxes (third term, vertical flux measured in our study). Note that the contribution of CO_2 exchange from the advective terms is often ignored or considered negligible during daytime, and at many sites during nighttime hours as well.

To assess the contribution of turbulent transport to net ecosystem exchange, we first assumed that the efficiency of turbulence to transport mass and energy could be represented by the magnitude of turbulent kinetic energy (TKE). We then defined two turbulence intensity parameters I_w and I_u based on the ratio of mean vertical ($\overline{w}$, m s^{-1}) or horizontal ($\overline{u}$, m s^{-1}) wind velocity to a modified turbulent velocity scale (u_{TKE}, m s^{-1}), where u_{TKE} is defined as,

$$u_{TKE} = \sqrt{(\overline{u'^2} + \overline{v'^2} + \overline{w'^2})} \quad (2)$$

and $\overline{u'^2}$, $\overline{v'^2}$ and $\overline{w'^2}$ are the mean variances in the stream-wise, cross-wise and vertical velocity directions, respectively. Note that u_{TKE} now has the same dimensions as the original velocity variables. We used a vertical turbulence intensity ratio,

$$I_w = \frac{\overline{w}}{u_{TKE}} \quad (3)$$

to determine conditions when transport by mean vertical wind flow (measured $\overline{w}$) could no longer be neglected compared to turbulent eddy flow; i.e., if I_w was greater than or equal to a critical I_w threshold (I_{wcrit}) then the mean vertical wind transport was considered non-negligible compared to turbulent exchange and the EC fluxes were gap-filled. Vertical velocity is hard to measure with a high degree of accuracy and is subject to errors associated with miss-leveling of the sonic anemometer. For these reasons we created tower-specific I_w thresholds and we made the assumption that no significant changes in the precision of $\overline{w}$ measurements occurred during the study period for any given anemometer.

A horizontal turbulence intensity ratio,

$$I_u = \frac{\overline{u}}{u_{TKE}} \quad (4)$$

was used to examine the contributions of transport by mean horizontal wind flow to turbulent eddy flow. If $I_u \geq I_{ucrit}$, advective transport of energy, mass and momentum was considered non-negligible compared to turbulent transport and the EC fluxes were gap-filled. We chose to use a modified turbulent velocity scale (u_{TKE}) instead of the commonly used surface friction velocity (u_*) to infer ABL stability conditions. In classical homogeneous turbulence with zero mean wind shear, turbulence would still transport scalars but u_* would by definition be zero. A turbulence scale

based on TKE takes into account both mechanical- and buoyancy-generated turbulence making it more appropriate to use during daytime as well as nighttime hours because u_* gives information on shear-generated turbulence only.

Friction velocity is routinely used in EC studies as a filter for identifying (and removing) CO_2 flux measurements taken during inadequate nighttime turbulence (called the "ustar-correction method", Goulden et al. 1996; also see Aubinet et al. 2000, Massman and Lee 2002, Gu et al. 2005, Papale et al. 2006). We argue that this application of friction velocity is not the most ideal because (1) intermittent, buoyancy-driven turbulence can also occur at night over complex terrain, and these periods of instability will not be captured by the u_* parameter, (2) the magnitude of u_* is time dependent such that u_* is well behaved during high frequency flow events but becomes problematic (due to high variance) under mesoscale flow (Acevedo et al. 2008), and (3) u_* is not an independent state variable when used as a filter for "accepting" CO_2 fluxes because it is calculated from the stream-wise and cross-wise momentum fluxes (Eqn. 5),

$$u_*^2 = \sqrt{(\overline{u'w'}^2 + \overline{v'w'}^2)} = \frac{\left|\tau_{Reynolds}\right|}{\overline{\rho}} \quad (5)$$

where the Reynolds shear stress is defined as,

$$\left|\tau_{Reynolds}\right| = \sqrt{(\tau_{uw}^2 + \tau_{vw}^2)} \quad (6)$$

While friction velocity is a flux and a result of the momentum sink, TKE is instead conceptually linked to the independent ability of turbulence to transfer mass and energy through the ABL. The velocity variances and standard deviations, and TKE-derived measures are all direct measures of turbulence.

3.3 Fetch, footprint and advection estimates

A simple, parameterized footprint model (Kljun et al. 2004, http://footprint.kljun.net/index.php) was used in criterion (6) to determine the extent of which measured turbulent fluxes were influenced by scalar sources outside of the early seral stands. A footprint size and shape varies according to receptor height (here the EC measurement height), surface or canopy roughness, and planetary boundary layer mixing conditions during which the fluxes were measured (i.e., the ratio of advective to turbulent transport). While the chosen model relies on a simplified scaling approach for the footprint functions, it has been thoroughly tested with a more complex 3-D Lagrangian stochastic footprint model (Kljun et al. 2002). The estimated footprint (x_R) is calculated using user-defined values of standard deviation of vertical wind velocity (σ_w), friction velocity (u_*), planetary boundary layer height (we used 1500 m during daytime and 600 m at nighttime), zero displacement height ($z_o = 0.10h_c$, where h_c is the canopy height) and EC measurement height. In this study all footprint estimates were based on x_R, the distance from the flux tower which includes 80% of the source area influencing the EC measurement. For the model runs, we separated all turbulence data first into daytime (10:00 – 14:00) and nighttime (24:00 – 2:00) classes, and secondly into wind direction sectors (eight 45º bins).

A vertical and horizontal advection measurement system for CO_2 and H_2O vapor was set-up for a couple of seasons at the 500-year old Wind River site as described in Paw U et al. (2004). Their study estimated that advection contributes between 10 to 20% of the above canopy flux at night at the old-growth forest (Paw U et al. 2004), although this contribution is predicted to vary depending on mean wind speed, canopy height and effective transfer coefficients (Park and Paw U 2004, Park 2006). Hour-to-hour advection was difficult to measure and because the

estimated contribution was relatively small we decided not to include measurement-based corrections for an advective component in the net ecosystem exchange.

3.4 Gap-filling and uncertainty analysis

Missing or excluded 30-minute F_{NEE} and λE measurements from the 3 flux tower time series were gap-filled using on-line algorithms from Reichstein et al. (2005) (http://gaia.agraria.unitus.it/database/eddyproc/). The gap-filling method uses both a mean diurnal approach and look-up tables for filling periods of missing data and is an advancement of the methodology described in Falge et al. (2001). λE data were gap-filled to estimate daily or monthly evapotranspiration (E_T, mm). The meteorological data were gap-filled using a similar mean diurnal approach. Uncertainty estimates in total E_T (kg H_2O m^{-2}) and monthly midday F_{NEE} (μmol m^{-2} s^{-1}) were assessed with bootstrapping simulations using the Monte Carlo approach (following Ma et al. 2007). Bootstrapping re-sampling was performed 5000 times on each of the daily time series and uncertainty estimates were based on the standard deviation of the simulations at the 90% confidence interval.

3.5 Energy budget and albedo

Energy budget closure was assessed at all stands using daytime, half-hour flux data during periods of good fetch, adequate turbulence and no precipitation. Energy budget closure was estimated from Eqn. 7,

$$H + \lambda E = R_n - G - S_e \quad (7)$$

Where R_n is net radiation (W m^{-2}), G is ground heat flux (W m^{-2}), and S_e is energy stored in biomass, canopy air space and soil above the ground heat flux plate (W m^{-2}). S_e was

calculated only at the old-growth stand and was assumed to be negligible in the short, low biomass canopies of the early seral stands. At the early seral stands ground heat flux was estimated using half-hourly changes in soil temperature from vertical soil temperature profiles. A midday Bowen ratio (β) was defined as the ratio of sensible heat to latent heat during half hours 10:00 – 14:00. β was used to asses what portion of available energy was transferred to sensible heat and how much to latent heat or evapotranspiration.

Albedo at the Wind River old-growth forest was estimated using incoming and outgoing shortwave radiation from a 4-stream radiometer mounted at a height of 85 meters on the canopy crane. Albedo at ESS07 was estimated from PAR-only wavelengths using up- and down-facing PAR sensors mounted at a height of 6 meters above ground level. Albedo was calculated for all half hours at ESS07 when incoming photosynthetic photon flux density (PPFD) > 100 μmol m^{-2} s^{-1} and at OG when incoming short-wave radiation > 50 W m^{-2} to eliminate errors caused by low solar elevation angles. At ESN, albedo was not measured directly but was estimated using the 16-day MODIS albedo product in 2006 (MOD43B3, http://edcdaac.usgs.gov/modis/mod43b3v4.asp).

3.6 LAI

LAI was indirectly measured at the early seral stands using digital hemispheric photography (DHP) and estimated using HemiView 2.1 (Delta-T Devices Ltd., Cambridge, UK) and Eqn 8 (Chen 1996, Chen et al. 1997),

$$LAI = \frac{(1-\alpha) LAI_{eff} \gamma E}{\Omega_E} \quad (8)$$

Where, LAI_{eff} is effective, single-sided LAI and was calculated using the software program based on DHP gap fraction, α is woody-to-plant ratio and was set at 0.20, γ_E is needle-to-shoot ratio

and was set at 1.61 and Ω_E is the foliage element clumping index and was set at 0.91. The three parameter values are based on measurement data from a 14 year old Douglas fir stand at Campbell River, British Columbia (Chen 1996, Chen et al. 2006). The hemispheric photos were taken at a height of 10 cm with a Nikon COOLPIX E4300 digital camera adapted with a Nikon Fisheye Converter lens. Fern and other ground species were cleared before the photos were taken to ensure that only trees were included in the canopy LAI estimates. Do to logistics DHP surveys were done just once at both sites. The photos were taken just past sunset on September 1, 2006 at ESN06 and August 30-31, 2007 at ESS07. At ESN06 15 images were taken along a 150 m west-to-east transect (centered at the flux tower) at 10 m intervals. At ESS07 17 images were taken along a 170 m west-to-east transect at 10 m intervals.

4. Results

4.1 Local meteorology

Meteorological data from the nearby NOAA station at the Carson Fish Hatchery showed that annual mean air temperature was near the long-term (1977-1997) mean (8.8 °C) in both 2006 (8.9 °C) and 2007 (8.7 °C). Total water-year (October through September) precipitation was also near average (2366 mm) in 2006 (2361 mm) and 2007 (2129 mm). Although 2006 and 2007 were very similar in terms of total precipitation and annual mean temperature, the spring and summer seasons were in fact climatologically distinct. Spring 2006 was cooler and wetter (409 mm) and led into a very dry (72 mm) and warm (17.2 °C) drought season. In 2007, the spring months were drier (217 mm) than in 2006 although late-season rains made the summer much wetter (316 mm) and cooler (16.4 °C). For comparison, the long-term averages for the drought season are 314 mm and 16.2 °C.

4.2 Site micrometeorology

Table 2 shows that the early seral stands were warmer and less humid than the dense old-growth forest during summer daylight hours (table 2). Average May-August VPD was 1.6 kPa at ESN06 and 1.2 kPa at OG06, and 1.3 kPa at ESS07 and 1.1 kPa at OG07 during the hours of 10:00-16:00. Soil moisture (θ_v) also varied amongst stands and years although the drought seasonal pattern remained a dominant feature. The near-surface (0-30 cm depth) θ_v was similar at both ESN06 and OG06: after June 2006 soil moisture began to steadily decrease and approached 0.15 m^3 m^{-3} until rains returned in October. At ESS07, 0-30 cm depth θ_v never dropped below 0.20 m^3 m^{-3} while it approached 0.15 m^3 m^{-3} at OG07. The additional measurement depths in 2007 revealed that while near-surface θ_v at OG07 fell below the critical

threshold of 0.2 m^3 m^{-3} for inducing ecosystem water stress (Falk et al. 2005, 2008), deeper θ_v in the rooting zone (1 to 1.5 meters) of old-growth trees never dropped below 0.3 m^3 m^{-3}. Daily maximum soil temperatures were higher at the early seral stands and temperature differences up to 15 °C were observed between ESS07 and OG07.

4.3 Early seral turbulence and footprint statistics

We observed fundamental differences between normalized (by mean daily maximum) mean wind speed (U), u_* and u_{TKE} depending on the time of day and site location (figure 2). At night, u_{TKE} and u_* were on average between 15-30% of their daily peak values (normalized u_* was significantly lower at ESN06) while the mean wind speed dropped below 30-35% of its maximum value only for a few hours before sunrise. Figure 2 also shows that u_{TKE} tends to be closer than u_* to the daily maximum during the morning to mid-afternoon hours while normalized u_* is greater in the late afternoon.

The critical horizontal threshold for insufficient turbulence was $I_{ucrit} = 2.5$ at ESN06 and $I_{ucrit} = 3$ at ESS07 (figs 3a & 4a). The critical vertical threshold for insufficient turbulence was $I_w \geq |0.20|$ at ESN06 and $I_w \geq |0.25|$ at ESS07 (figures 3b & 4b). To determine these thresholds we used a combination of footprint modeling (I_w and I_u values beyond which the flux footprint continuously extended outside the clear-cut stands) and flux statistics (I_u value beyond which the fluxes "leveled-off" or systematically approached zero). For example, when $I_u \geq I_{ucrit}$ mean midday F_{NEE} was 0.73 µmol m^{-2} s^{-1} at ESN06 and -0.51 µmol m^{-2} s^{-1} at ESS07. To test the robustness of our new parameters we also examined whether the turbulent flux statistics were sensitive to a critical turbulence threshold was based on u_* or u_{TKE}. Figure 5 illustrates that a greater number of "real" H fluxes would be excluded from the data series if a critical turbulence

threshold was based on u_* rather than u_{TKE}. 15% of sensible heat fluxes (mean = 16 W m^{-2}) were excluded using an u_{TKE} critical threshold while nearly 25% (mean H = 46 W m^{-2}) were excluded using the u_* critical approach. Data in figure 5 were binned into net radiation classes to show that H fluxes > 100 Wm^{-2} at very low u_* conditions (boxed gray regions) are probably true sensible heat fluxes since net radiation during these times was often greater than 400 W m^{-2}. The average half-hour in the boxed region in figure 5a was 12:00 and all boxed half-hours occurred between 8:00-18:00. Mean values for the boxed region data in figure 5a include: H = 145 W m^{-2}, u_* = 0.11 m s^{-1}, u_{TKE} = 0.98 m s^{-1}, U = 0.96 m s^{-1}, and I_u = 0.98. $I_u \leq I_{ucrit} = 3$ so the same sensible heat fluxes were not excluded using the I_u threshold approach which also considers buoyancy-produced turbulence (figure 5b).

The boxed sections in figures 3 and 4 show conditions when the mean flow contribution (i.e., advection from Trout Creek Hill) could no longer be a neglected component of the flux. Non-negligible horizontal mean flow was more prevalent at ESN06 during nighttime hours than non-negligible vertical mean flow (frequency of 24 to1), while non-negligible vertical mean flow and horizontal mean flow conditions occurred in roughly equal frequencies at ESS07. Also, non-negligible horizontal mean flow ($I_u \geq 2.5$) was occasionally observed (1.8% frequency) at ESN06 during daylight hours (figure 3a) but not at ESS07 as very few daylight hours (< 0.2 %) approached I_{ucrit} (figure 4a). Nighttime (2:00 – 4:00) flux footprints (x_R) extended at least 350 m in the westerly direction and went beyond the boundaries of both clear-cuts during high I_w and I_u conditions. Nighttime fluxes measured while I_w and I_u were less than I_{wcrit} and I_{ucrit} came from scalar sources closer to the towers (at least 200 m) but the flux footprints were still beyond the boundaries of the stands for most wind directions (82% and 85% of the time at ESN and ESS, respectively). For this reason and because I_w and I_u went beyond the critical thresholds an

1 additional 3% of the time at ESN and 11% at ESS, we do not include estimates of nighttime
2 ecosystem exchange in this paper.
3 Midday (10:00 – 14:00) footprints (x_R) ranged from 75 m (east upwind direction) to 100
4 m (north upwind direction) at ESN06 and 77 m (east upwind direction) to 115 m (north upwind
5 direction) at ESS07, translating into fetch-EC instrument ratios of 14:1 to 23:1. Available
6 fetch:EC instrument ratios averaged 33:1 and 34:1 at ESN and ESS, respectively, but ranged
7 from 10:1 to 44:1 depending on wind direction (table 3). Most wind directions at ESN06
8 included footprints within the clear-cut stand. Greatest uncertainty arose when winds were from
9 the southeasterly direction (23% of the data points) because footprints extended outside of the
10 clear-cut into an adjacent 80-year old Douglas-fir forest. These fluxes were removed from the
11 time series and gap-filled. Daytime footprints were less of a concern at ESS07 as nearly all
12 upwind directions had sufficient fetch. The only exception was when winds arose from the
13 northerly and southerly directions but this occurred less than 15% of the time.
14
15 *4.4 Energy balance and albedo*
16 Mean midday (10:00-14:00) energy fluxes and albedo estimates are listed in table 4 and
17 show energy exchange during the beginning, middle, and end of the drought seasons. Early
18 Seral North energy budget closure (EBC) was 81% ($R^2 = 0.93$) during mid-June to mid-
19 September in 2006 and slightly lower (79%, $R^2 = 0.89$) at ESS during the same period in 2007.
20 During the summer months old-growth EBC was 76% ($R^2 = 0.67$) in 2006 and 73% ($R^2 = 0.62$)
21 in 2007. Available energy was partitioned into 40% sensible heat and 41% latent heat at ESN
22 during the 2006 summer with 19% of the available energy unaccounted for, although table 4
23 shows high month-to-month variability in the energy partitioning variable β. At ESS 45% of

available energy was partitioned into sensible heat and 34% into latent heat with 21% unaccounted for. Higher Bowen ratios were measured at the old-growth stand than at either early seral forest. April-August mean midday β was 2.2 ± 0.9 at OG06 and 1.5 ± 0.6 at ESN06, and 2.0 ± 1.2 at OG07 and 1.2 ± 0.6 at ESS07. The largest site differences were measured in July during both years. Mean July β was 2.6 ± 1.0 at OG06 and 0.78 ± 0.3 at ESN06, and 2.2 ± 1.4 at OG07 and 0.94 ± 0.8 at ESS07. The low β ratios at the early seral sites in mid-summer are due to large latent heat fluxes. Ground heat storage accounted for less than 1% of the available net energy at the old-growth stand. In the more open canopies at the early seral stands ground heat storage was 8% to 15% of the available energy. Albedo was higher at the open early seral stands (12% - 15%) than at the old-growth forest (7% - 8%). A summer decline in albedo was not observed at OG but was observed at ESS07. PAR albedo declined from 14.9% in May to 12.9% in October at Early Seral South following structural canopy changes including bud break and fern growth (figure 6). No significant changes in albedo were measured at the old-growth stand in 2006 or 2007.

4.5 Seasonal and monthly flux dynamics

Midday (10:00-14:00) CO_2 fluxes peaked seasonally in April at the old-growth stand and were -14.0 ± 3.4 μmol m^{-2} s^{-1} in 2006 and -12.3 ± 2.1 μmol m^{-2} s^{-1} in 2007 (figure 7 a&b). In contrast, April midday F_{NEE} magnitudes were significantly ($P<0.0001$) smaller (less net carbon uptake) at the early seral stands, - 4.0 ± 1.4 μmol m^{-2} s^{-1} at ESN06 and - 3.8 ± 1.3 μmol m^{-2} s^{-1} at ESS07, and we observed peak midday CO_2 fluxes not until two to three months later. Maximum net CO_2 uptake rates were measured in July at ESN06 (-10.2 ± 2.0 μmol m^{-2} s^{-1}) and in June at ESS07 (-8.7 ± 0.9 μmol m^{-2} s^{-1}) while net CO_2 uptake dropped sharply in June at the old-growth

forest and continued to decline throughout the summer in both 2006 and 2007. E_T was relatively constant between April and June at the OG stand and a seasonal-summer decline was not observed until July in 2006 and August in 2007 (figure 7 c&d). Strongest E_T seasonality was observed at ESN. June-August E_T averaged 85 mm mo^{-1} while April-May E_T was 40 mm lower. Not enough data were available at ESS to make the same seasonal comparisons. Total May through August E_T was 305 ± 11 mm at ESN06 and 231± 9 mm at OG06, and 289 ± 9 mm at ESS07 and 230 ± 8 mm at OG07.

We found a strong correlation between monthly midday Bowen ratio and midday F_{NEE} at the early seral stands ($R^2 = 0.92$ in 2006 and $R^2 = 0.82$ in 2007) so that higher β were associated with less negative CO_2 fluxes. This relationship was also observed at the old-growth stand in 2007 ($R^2 = 0.50$) although a link was not observed in 2006 ($R^2 = 0.00$). Figure 8 shows the correlation between β and F_{NEE} for ESS07 and OG07. Note that the positive relationship between β and F_{NEE} breaks down during the month of May at OG07. This month was relatively dry and warm, experienced moderate VPD but had plentiful below-surface soil moisture. This combination of factors produced a relatively high Bowen ratio and larger negative (more net carbon uptake) CO_2 fluxes at the old-growth stand while CO_2 fluxes at the early seral stands were significantly less negative (less net carbon uptake).

5. Discussion and conclusions

Before we could confidently compare fluxes amongst stands we first needed to answer the following question: were the clear-cut patches large enough in size so that flux measurements were representative of the vegetation of interest? We were not satisfied that the friction velocity scale was able indicate periods of inadequate turbulent mixing during both daytime and nighttime hours at the early seral stands so we created new parameters I_w and I_u. Our turbulence-intensity methodology for the early seral stands revealed that most of the nighttime CO_2 fluxes were measured during non-negligible vertical mean flow, non-negligible horizontal mean flow or from scalar sources outside the boundaries of the clear-cuts. These findings support the theoretical calculations found in Park and Paw U (2004) and Park 2006 that predict significant advection along abrupt forest edges. We decided to not include any nighttime CO_2 flux data in this paper because we believed that the EC technique was not accurately measuring turbulent CO_2 exchange at night (i.e., respiration flux). For consistency we also did not include any nighttime data at the old-growth site. Other clear-cut studies have reported nighttime flux data including Kolari et al. (2004) and Humphreys et al. (2005). Kolari et al. (2004) were able to use 41% of their nighttime flux data based on a u_* critical value of 0.2 m s^{-1} in a 7 hectare clear-cut that had maximum fetch of 200 m, while Humphreys et al. 2005 found that nighttime F_{NEE} was no longer positively correlated with u_* after a threshold of 0.08 m s^{-1} was reached and were able to keep 80% of the nighttime data from a clear-cut flux tower. We suggest two primary reasons for why we rejected our nighttime flux data:

(1) *Differences in footprint and fetch*: Wind River ES tree height and high growth rates required that we measure at least 5 m above the ground surface and in doing so we increased the footprint size so that it often extended beyond the stand boundaries. Humphreys et al. 2005 in

comparison measured over a younger, shorter and smoother Douglas-fir canopy which shifted the turbulence frequency distribution towards smaller eddies which requires smaller footprints to resolve. Footprint issues are not an uncommon feature for forest flux studies particularly since most EC towers are now located in non-homogeneous terrain (Gockede et al. 2008). Additionally, our early seral stands had a drastic rough-to-smooth surface change (the transition from a 40 meter, 80 year old forest to 4 meter, 10 year old forest) which increased the fetch required to ensure that we were measuring within the atmospheric equilibrium layer. Our fetch:instrument height ratios were close to 35:1 for wind directions with adequate fetch. This is slightly less than the general 40:1 rule although close to ratios used in similar clear-cut studies (van Breugel et al. 1999, Kolari et al. 2004).

(2) *Differences in turbulence methodology*: This paper introduced a novel method to determine adequate turbulent conditions for flux measurements. We suggest that a velocity scale based on TKE (e.g., u_{TKE}) is a better way to assess ABL mixing because it includes turbulence generated by buoyancy as well as from mechanical forces. Also, turbulence regimes based on a u_* scale can be misclassified during mesoscale flows while a TKE-based scale does not suffer from the same time-dependent variance errors (Acevedo et al. 2008). When the mass budget exchange equations, such as presented in Lee (1998), Paw U et al. (2000), and Park and Paw U (2004) are carefully examined, it is clear that the kinematics of turbulent transport are related to the velocity fluctuations (in this case, as measured by u_{TKE}) and the kinematics of advective transport are driven by the mean velocity field. The ratio to assess the importance of turbulence compared to horizontal or vertical advection used here is a form of the dimensionless number for a particular site (xK/Uh_c^2), which is shown in Park and Paw U (2004) and Park (2007) to be related theoretically to the ratio of turbulent exchange to mean advective exchange. The distance (fetch) is x, the turbulent transport coefficient is K, U is the mean wind speed and h_c is the canopy height. The relationship

between these two ratios can be gleaned by parameterizing K as a constant multiplied by a turbulent fluctuation, represented by u_{TKE}, and recognizing that the ratio (x/h_c^2) is a constant for any given site and measurement location. Hence, the reciprocal of our ratio used here, multiplied by constants, then is equivalent to the Park and Paw U (2004) dimensionless number.

The daytime EC data in this study were carefully screened by assessing footprint models, mean velocity-to-turbulence flow ratios and energy budget closure, and we feel confident in reporting a high fraction of daytime ecosystem fluxes from the early seral stands. Continuous failure to close the energy budget ($H + \lambda E < R_n - G - S_e$) during the daytime hours can indicate systematic underestimation of the turbulent eddy fluxes (Foken 2008) but 80% energy closure at the ES stands suggests that daytime fluxes were not largely underestimated and the energy closure percentages are on average with other FLUXNET sites (Wilson et al. 2002a). 28% and 13% of the daytime data at ESN and ESS, respectively, occurred when the footprint model indicated inadequate fetch and these data points were removed. I_u and I_w went beyond the critical thresholds occasionally during daylight hours and our data correspond with studies by Feigenwinter et al. (2004) and Marcolla et al. (2005) which show that midday advective fluxes can make up to 10% of the eddy flux. Although these studies and our data suggest that vertical advection is present in clear-cuts, datasets that show this are still extremely limited (Belcher et al. 2008).

The relationship between PAR albedo and LAI has shown to be significant for low LAI ecosystems (e.g., Ryu et al. 2008). Here we used changes in PAR albedo over weekly periods to track LAI changes at ESS since we did not have temporal LAI measurements. PAR albedo declined by nearly 3% from May through October as the ESS canopy developed after bud break (May 10-28) and from prolific bracken fern growth (> 50% ground coverage in June, July and August) (figure 6). Terminal bud break in Pacific Northwest Douglas-fir trees occurs in late

spring to early summer and the production of new needles as well as the summer-time growth of ground species has fundamental impacts on a forest with very low biomass (LAI ~ 1 to 2 m^2 m^{-2}). At the old-growth forest phenological changes appeared to not significantly increase net carbon uptake as we observed maximum uptake rates in April. Peak carbon uptake during spring-time has also been observed at an old-growth Ponderosa pine forest in central Oregon (Law et al. 2000) and at a intermediate-age coastal Douglas-fir ecosystem on Vancouver Island, British Columbia (Humphreys et al. 2006), and may be a universal trait of intermediate to mature conifer forests. As with Wind River these sites experience strong wet/cool and dry/warm seasonality although the summers are much drier and warmer at the Oregon site and cooler and wetter at the Vancouver Island forest than at Wind River.

If we add Douglas-fir data from British Columbia to our dataset then an additional age class (0-3 years, initiation seral) is available for our stand-age discussion on CO_2 fluxes. Figure 9 summarizes Pacific Northwest Douglas-fir EC data and shows how midday, July-September F_{NEE} differ by stand age. Within the Wind River chronosequence, highest to lowest late summer net carbon uptake rates have been measured in the 40-year old stand, 20-year old stand, early seral stands (~10 years old), and old-growth stand. The initiation seral stage shows smaller but still net CO_2 uptake during summer-time midday hours.

Old-growth E_T varied little (Δ=3 mm) between the 2006 and 2007 summer months even though rainfall and average θ_v showed that 2007 was wetter. While it is true that there is some uncertainty involved with E_T measurements, the uncertainty should remain the same from year to year at each site as long as the IRGA is carefully calibrated. We inadvertently introduced different instrument-related errors by using a closed-path IRGA at the old-growth stand and an open-path IRGA at the early seral stands. In lieu of assessing the instrument errors directly, we

used bootstrapping to quantify uncertainties on E_T. This showed that E_T from the early seral stands and the old-growth forest were significantly different. The evapotranspiration and Bowen ratio measurements presented here are somewhat unique compared to other stand-age studies because we report higher E_T and lower β at the youngest sites. For example, Anthoni et al. 2002 measured E_T over a 15 year old and a mixed-age old-growth Ponderosa pine forest during the 2000 summer drought season and reported lower E_T over the younger stand even though weather anomalies were similar at both sites. Considering our stand-age site differences it is worth noting that a wide range of summer-time β (0.46 to 2.2, mean = 1.1) have been published for conifer forests (Wilson et al. 2002b) and variability can be high even within the same study site because β varies dramatically depending on the wetness of the canopy. Humphreys et al. (2003) reported a mean summer-time β of 1.1 at the intermediate-age Douglas-fir, Vancouver Island stand in 1998 although monthly mean values ranged from 0.8 to 1.91 and even broader ranges were observed over a 24-hour or weekly period.

Our paper reports crucial data for the early seral age class for understanding how stand-age affects flux exchange. While other EC studies have shown that net carbon uptake is greater in mature conifer stands than in the 0-20 year age class, we stress that our flux data show how highly variable this youngest age class is to weather and phenological events. Our study also sheds light on how important it is to filter even daytime fluxes based on footprint estimates and ABL turbulence statistics in small clear-cut stands to ensure that eddy covariance theory is valid.

Acknowledgements

SW would like to thank Mark Creighton and Annie Hamilton at the Wind River Canopy Crane Facility for their hospitality and assistance throughout this project. The authors also thank Drs. Dennis Baldocchi (UC Berkeley), Julie Lundquist (LLNL) and Susan Ustin (UC Davis) for their technical advice and help in the preparation of this manuscript. In addition, gratitude goes to the two anonymous reviewers whose comments were critical for improving this paper. This research was supported by the Office of Science (BER), US Department of Energy, through the Western Regional Center of the National Institute for Global Environmental Change (Cooperative Agreement NO. DE-FC03-90ER61010), and the Jastro Shields Graduate Research Scholarship (UC Davis). Any opinions, findings and conclusions or recommendations expressed herein are those of the authors and do not necessarily reflect the view of the DOE. The Wind River Canopy Crane Research Facility is operated under joint sponsorship of the University of Washington and the USDA Forest Service/PNW Station and we acknowledge both for significant support. Lawrence Livermore National Laboratory is operated by Lawrence Livermore National Security, LLC, for the U.S. Department of Energy, National Nuclear Security Administration under Contract DE-AC52-07NA27344.

References

Amiro, B.D., Barr, A.G., Black, T.A. et al. (2006) Carbon, energy and water fluxes at mature and disturbed forest sites, Saskatchewan, Canada. Agric. For. Meteorol. 136, 237-251.

Anthoni, P.M., Unsworth, M.H., Law, B.E., Irvine, J., Baldocchi, D.D., van Tuyl, S., Moore, D. (2002) Seasonal differences in carbon and water vapor exchange in young and old-growth ponderosa pine ecosystems. Agric. For. Meteorol. 111, 203-222.

Acevedo, O.C., Moraes, O.L., Degrazia, G.A., Fitzjarrald, D.R., Manzi, A.O., Campos, J.G. (2008) Is friction velocity the most appropriate scale for correcting nocturnal carbon dioxide fluxes? Agric. For. Meteorol. in press.

Aubinet, M., Grelle, A., Ibrom, A. et al. (2000) Estimates of the annual net carbon and water exchange of forests: The EUROFLUX methodology. Advances Ecol. Res. 30, 113-175.

Bauerle, W.L., Hinckley, T.M., Cermak, J., Kucera, J. (1999) The canopy water relations of old-growth Douglas-fir trees. Trees 13, 211-217.

Belcher, S.E., Finnigan, J.J., Harman, I.N. (2008) Flows through forest canopies in complex terrain. Ecological Applications 18: 1436-1453.

Chen, J.M. (1996) Optically-based methods for measuring seasonal variation in leaf area index of boreal conifer forests. Agric. For. Meteorol. 80, 135-163.

Chen, J.M., Rich, P.M., Gower, S.T., Norman, J.M., Plummer, S. (1997) Leaf area index of boreal forests: theory, techniques, and measurements. J. Geophys. Res. 102(D24), 29429-29443.

Chen, J.M., Govind, A., Sonnentag, O., Zhang, Y., Barr, A., Amiro, B. (2006) Leaf area index measurements at Fluxnet-Canada forest sites. Agric. For. Meteorol. 140, 257-268.

Chen, J.Q., Falk, M., Euskirchen, E. et al. (2002) Biophysical controls on carbon flows in three successional Douglas-fir stands based on eddy-covariance measurements. Tree Physiol. 22, 169-177.

Chen, J.Q., Paw U, K.T., Ustin, S.L., Suchanek, T.H., Bond, B.J., Brosofske, K.D., Falk, M. (2004) Net ecosystem exchanges of carbon, water, and energy in young and old-growth Douglas-fir forests. Ecosystems 7, 534-544.

Cohen, W.B., Harmon, M.E., Wallin, D.O., Fiorella, M. (1996) Two decades of carbon flux from forests of the Pacific Northwest. Bioscience 46, 836-844.

Falge, E., Baldocchi, D., Olson, R., et al (2001) Gap filling strategies for defensible annual sums of net ecosystem exchange. Agric. For. Meteorol. 107, 43-69

Falk, M. (2005) Carbon and energy exchange between an old-growth forest and the atmosphere. Ph.D. Dissertation, University of California, Davis, California, pp 196.

Falk, M., Paw U, K.T., Wharton, S., Schroeder, M. (2005) Is soil respiration a major contributor to the carbon budget within a Pacific Northwest old-growth forest? Agric. For. Meteorol. 135, 269-283.

Falk, M., Wharton, S., Schroeder, M., Ustin, S., Paw U, K.T. (2008) Flux partitioning in an old growth forest: seasonal and interannual dynamics. Tree Physiol. 28, 509-520.

Feigenwinter, C.C., Bernhofer, C., Vogt, R. (2004) The influence of advection on the short-term CO2 budget in and above a forest canopy. Boundary-Layer Meteorol. 113, 201-224.

Foken, T. (2008) The energy balance closure problem: an overview. Ecological Applications 18:1351-1367.

Gockede, M., Foken, T., Aubinet, M. et al. (2008). Quality control of CarboEurope flux data – Part 1: coupling footprint analyses with flux data quality assessment to evaluate sites in forest ecosystems. Biogeosciences 5, 433-450.

Goulden, M.L., Munger, J.W., Fan, S.-M., Daube, B.C., Wofsy, S.C. (1996) Measurements of carbon sequestration by long-term eddy covariance measurements and a critical evaluation of accuracy. Global Change Biol. 2, 169-182.

Grier, C. C. and R. S. Logan. (1977) Old-growth *Pseudotsuga menziesii* communities of a western Oregon watershed: biomass distribution and production budgets. Ecological Monographs 47, 373-400.

Gu, L.H., Falge. E., Baldocchi, D. et al. (2005) Objective threshold determination for nighttime eddy flux filtering. Ag. For. Meteor. 128, 179-197.

Harmon, M.E., Bible, K., Ryan, M.G., Shaw, D.C., Chen, H., Klopatek, J., Li, X. (2004) Production, respiration, and overall carbon balance in an old-growth *Pseudotsuga-Tsuga* forest ecosystem. Ecosystems 7, 498-512.

Humphreys, E.R., Black, T., Ethier, G., Drewitt, G., Spittlehouse, D., Jork, E., Nesic, Z., Livingston, N. (2003) Annual and seasonal variability of sensible and latent heat fluxes above a coastal Douglas-fir forest, British Columbia, Canada. Agric. For. Meteorol. 115, 109-125.

Humphreys, E.R., Andrew Black, T., Morgenstern, K., Li, Z., Nesic, Z. (2005) Net ecosystem production of a Douglas-fir stand for 3 years following clearcut harvesting. Global Change Biol. 11, 450-464.

Humphreys, E.R., Black, T.A., Morgenstern, K., Cai T., Drewitt, G.B., Nesic, Z., Trofymow, J.A. (2006) Carbon dioxide fluxes in coastal Douglas-fir stands of different stages of development after clearcut harvesting. Agric. For. Meteorol. 140, 6-22.

Irvine, M.R., Gardiner, B.A., Hill, M.K. (1997) The evolution of turbulence across a forest edge. Boundary-Layer Meteorol. 84, 467-486.

Irvine, J., Law B.E., Anthoni, P.M., Meinzer, F.C. (2002) Water limitations to carbon exchange in old-growth and young ponderosa pine stands. Tree Physiol. 22, 189- 196.

Kljun, N., Rotach, M.W., Schmid, H.P. (2002) A 3D backward Lagrangian footprint model for a wide range of boundary layer stratifications. Boundary-Layer Meteorol. 103, 205-226.

Kljun, N., Calanca, P., Rotach, M.W., Schmid, H.P. (2004) A simple parameterization for flux footprint predictions. Boundary-Layer Meteorol. 112, 503-523.

Klopatek, J.M. (2002) Belowground carbon pools and processes in different age stands of Douglas-fir. Tree Physiol. 22, 197-204.

Klopatek, J.M., Barry, M.J., Johnson, D.W. (2006) Potential canopy interception of nitrogen in the Pacific Northwest, USA. For. Ecol. Manag. 234, 344-354.

Kolari, P., Pumpanen, J., Rannik, U., Ilvesniemi, H., Hari P., Berninger, F. (2004) Carbon balance of different aged Scots pine forests in Southern Finland. Global Change Biol. 10, 1106-1119.

Kruijt, B. (1994) Turbulence over forests, downwind of an edge. Ph.D. Dissertation, University of Groningen.

Law, B.E., Williams, M., Anthoni, P.M., Baldocchi, D.D., Unsworth, M.H. (2000) Measuring and modeling seasonal variation of carbon dioxide and water vapour exchange of a *Pinus ponderosa* forest subject to soil water deficit. Global Change Biol. 6, 613-630.

Law, B.E. Sun, O.J., Campbell, J., Van Tuyl, S., Thornton, P.E. (2003) Changes in carbon storage and fluxes in a chronosequence of ponderosa pine. Global Change Biol. 9, 510-524.

Lee, X.H. (1998) On micrometeorological observations of surface-air exchange over tall vegetation. Agric. For. Meteorol. 91, 39-49.

Ma, S., Baldocchi, D.D., Xu, L., Hehn, T. (2007) Inter-annual variability in carbon dioxide exchange of an oak/grass savanna and open grassland in California. Agric. For. Meteorol. 147, 157-171.

Marcolla, B., Cescatti, A., Monyagnani, L, Manca, G. Kerschbaumer, G., Minerbi, S. (2005) Importance of advection in the atmospheric exchanges of an alpine forest. Agric. For. Meteorol. 130, 193-206.

Massman, W.J. and X. Lee. (2002) Eddy covariance flux corrections and uncertainties in long-

term studies of carbon and energy exchanges. Ag. For. Meteor. 113, 121-144.

McDowell, N.G., Licata, J., Bond, B.J. (2005) Environmental sensitivity of gas exchange in different-sized trees. Oecologia 145, 9-20.

Oak Ridge National Laboratory Distributed Active Archive Center (ORNL-DAAC) (2007) MODIS subsetted land products, Collection 4. Available on-line [http://www.daac.ornl.gov/MODIS/modis.html] from ORNL-DAAC, Oak Ridge, Tennessee, USA. Accessed October, 2007.

Papale, D., Reichstein, M., Aubinet, M., et al. (2006) Towards a standardized processing of net ecosystem exchange measured with eddy covariance technique: algorithms and uncertainty estimation. Biogeosciences 3, 571-583.

Park, Y.-S. (2006) Numerical study of scalar advection in canopies using a higher-order closure model. Ph.D. Dissertation, Univ. of California, Davis, 123 p.

Park, Y.-S. and Paw U, K.T. (2004) Numerical estimations of horizontal advection inside canopies. J. Applied Meteorol. 43, 1530-1538.

Parker, G.S., Chen, J., Harmon, M.E., Lefsky, M.A., Shaw, D.C., Thomas, S.C., Weiss, S.B., van Pelt, R., Winner, W.E. (2004) Three-dimensional structure of the old-growth *Pseudotsuga-*

tsuga canopy and its implications for radiation balance, microclimate, and gas exchange. Ecosystems 7, 440-453.

Paw U, K.T., Baldocchi, D., Meyers, T.P., and Wilson, K.B. (2000) Correction of eddy-covariance measurements incorporating both advective effects and density fluxes. Boundary-Layer Meteorol. 91, 487-511.

Paw U, K.T., Falk, M., Suchanek, T.H., et al. (2004) Carbon dioxide exchange between an old-growth forest and the atmosphere. Ecosystems 7, 513-524.

Phillips, N., Bond, B.J., McDowell, N, Ryan, M.G. (2002) Canopy and hydraulic conductance in young, mature and old Douglas-fir trees. Tree Physiol. 22, 205-211.

Reichstein, M., Falge, E., Baldocchi, D. et al. (2005) On the separation of net ecosystem exchange into assimilation and ecosystem respiration: review and improved algorithm. Global Change Biol. 11, 1424-1439.

Ryu, Y., Baldocchi, D.D., Ma, S., Hehn, T. (2008) Interannual variability of evapotranspiration and energy exchange over an annual grassland in California. J. Geophys. Res. 113(D9), D09104, doi:10.1029/2007JD009263.

Sachs, L. (1996) Angewandte Statistik: Anwendung Statistischer Methoden, Springer, Berlin.

Schmid, H.P. (1994) Source area for scalars and scalar fluxes. Boundary-Layer Meteorol. 67, 293-318.

Shaw, D.C., J.F. Franklin, K. Bible, J. Klopatek, E. Freeman, S. Greene, G.G. Parker (2004) Ecological setting of the Wind River old-growth forest. Ecosystems 7, 427-439.

Song, C. and C.E. Woodcock (2002) Effects of stand age structure on regional carbon budgets of forest ecosystems. Eos Trans. AGU, 83(47), Fall Meet. Suppl., Abstract B12B-0812.

Thomas, S.C. and Winner, W.E. (2000) Leaf area index of an old-growth Douglas-fir forest estimated from direct structural measurements in the canopy. Can. J. For. Res. 30, 1922-1930.

Thomas, S.C. and Winner, W.E. (2002) Photosynthetic differences between saplings and adult trees: an integration of field results by meta-analysis. Tree Physiol. 22, 117-127.

Unsworth, M.H., Phillips, N., Link, T. et al. (2004) Components and controls of water flux in an old-growth Douglas-fir-western hemlock ecosystem. Ecosystems 7, 468-481.

van Breugel, P.B., Klaassen, W., Moors, E.J. (1999) Fetch requirements near a forest edge. Phys Chem Earth (B), 24, 125-131.

Webb, E.K., Pearman, G.I., Leuning, R. (1980) Correction of flux measurements for density effects due to heat and water-vapor transfer. Quart. J. Roy. Meteorol. Soc. 106, 85-100.

Wilson, K., Goldstein, A., Falge, E. et al. (2002a) Energy balance closure at FLUXNET sites. Agric. For. Meteorol. 113, 223-243.

Wilson, K.B., Baldocchi, D.D., Aubinet, M. et al. (2002b) Energy partitioning between latent and sensible heat flux during the warm season at FLUXNET sites. Water Resources Research 38, doi:10.1029/2001WR000989.

Wilson, J. and Swaters, G. (1991) The source area influencing a measurement in the PBL: "the footprint", Boundary-Layer Meteor. 55, 25-46.

Winner, W.E., Thomas, S.C., Berry, J.A. et al. (2004) Canopy carbon gain and water use: analysis of old-growth conifers in the Pacific Northwest. Ecosystems 7, 482-497.

Table Headings

Table 1. Stand characteristics and flux tower descriptions. *Percentage of daylight hours with missing data or data excluded through post-processing during the measurement period.

Table 2. A comparison of micrometeorological conditions at the flux towers for the months of April through September. ¨ = incomplete data. *Hours 10:00-16:00 only.

Table 3. Daytime fetch requirements and availability by wind direction at the early seral flux towers. The shaded region shows the percentage of the time when adequate fetch was available, and during those periods the mean fetch:instrument height ratio from footprint modeling and the calculated mean fetch:instrument height ratio at each early seral tower.

Table 4. Mean midday net radiation, soil heat flux, Bowen ratio and albedo measurements for three months (early drought-, mid drought- and late drought-season) at the 3 flux towers. NA = not available.

Figure Headings

Figure 1. Location of the canopy crane and 2 early seral flux towers in the Gifford Pinchot National Forest, Southern Washington.

Figure 2. Mean diurnal plots for mean wind speed, u_* and u_{TKE} normalized by each series' daily maxima at ESN 2006 (a) and ESS 2007 (b) which show at what hour of the day the largest and smallest magnitudes of each variable are present.

Figure 3. Half-hourly horizontal mean flow-to-turbulence intensity ratios (a) and vertical mean flow-to-turbulence ratios (b) for both daytime and nighttime hours at ESN in 2006 by wind direction. The boxed regions show non-negligible, horizontal mean flow (and possible advection) coming from the direction of Trout Creek Hill.

Figure 4. Half-hourly horizontal mean flow-to-turbulence intensity ratios (a) and vertical mean flow-to-turbulence ratios (b) for both daytime and nighttime hours at ESS in 2007 by wind direction. The boxed regions show non-negligible, nighttime horizontal and vertical mean flow (and possible advection) coming from the direction Trout Creek Hill.

Figure 5. Daytime sensible heat fluxes binned by net radiation and corresponding turbulence conditions shown by u_* (4a) or u_{TKE} (4b). The dashed line shows a critical turbulence threshold based on the lowest 15% turbulence intensity. The gray boxes highlight H fluxes > 100 W m^{-2} during critically low turbulent conditions.

Figure 6. Time series of weekly PAR-albedo (a) and midday F_{NEE} (b) along with the timing of major phenological events at Early Seral South from April through October, 2007. The dashed lines are seasonal mean albedo and mean F_{NEE}.

Figure 7. Mean midday CO_2 fluxes by month at Early Seral North and Old-Growth (2006) (a) and Early Seral South and Old-Growth (2007) (b). Total monthly E_T at ESN and OG06 (c) and ESS and OG07 (d). Uncertainties in the monthly values are also shown.

Figure 8. Monthly midday Bowen ratio and CO_2 flux at ESN and OG in 2006 (a) and ESS and OG in 2007 (b). Months are labeled numerically. The error bars are based on one standard deviation from the mean.

Figure 9. Carbon exchange data from a Douglas-fir flux tower chronosequence. Plotted are summer-time mean midday F_{NEE} (open squares are means) at the Wind River early seral stands (~10 year old, measured in 2006 and 2007), 20-year old stand (measured in 1999), 40-year old stand (measured in 1998) and old-growth forest, and the Vancouver Island initiation seral stand (2-3 years old, measured in 2002 and 2003). The years plotted for the old-growth stand are 1998, 1999, 2006 and 2007. The 20-year and 40-year stand data are approximated from Chen et al. (2004). The initiation stand data are approximated from Humphreys et al. (2005).

	Early Seral North	**Early Seral South**	**Old-Growth Stand**
Measurement period			
2006	Mar 27 - Oct 25		Mar 1 – Oct 31
2007		Apr 14 – Aug 31	Mar 1 – Oct 31
Gap-filled data			
EC flux*	24%	25%	16% (2006) 11% (2007)
Micro-Meteorological	29%	4%	1% (2006) 1% (2007)
Stand properties			
Maximum tree age	10	14	~ 450-500
Stand area (ha)	7	10	478
Slope	< 10 %	< 5 %	3.5 %
Site Preparation	minimal: abundant coarse woody debris (CWD): snags, logs	extensive: no CWD, mechanically homogenized soil to 1 m	none: natural fire recovery
Mean h_c (m)	4.4	3.6	55-65
LAI (m^2 m^{-2})	1.1 – 1.8	0.6 – 1.1	8.2 – 9.2 (Parker et al. 2002)
Foliar N %; Foliar C:N	1.2; 44:1 ± 3	1.4; 37:1 ± 3	1.2; 41:1 (Klopatek et al. 2006)
Soil properties			
Soil sand: silt: clay	66:28:6	62:29:9	60:31:9 (Shaw et al. 2004)
Soil C:N	27:1 ± 6	26:1 ± 3	25:1 ± 1 (Klopatek 2002)
Soil bulk density (g cm^{-3})	0.94	1.07	0.83

Table 1

1

	Ta_{max} (° C)	Ta_{min} (° C)	VPD* (kPa)	θ_v (m^3 m^{-3})	Ta_{max} (° C)	Ta_{min} (° C)	VPD* (kPa)	θ_v (m^3 m^{-3})	P (mm)
2006	**Early Seral North**				**Old-Growth**				**CFH**
April	--	--	--	--	13.7	3.2	0.5	--	112.3
May	20.0	9.5	1.1	0.33	18.6	7.4	0.9	0.34	59.2
June	25.8	9.2	1.8	0.31	22.0	11.2	1.0	0.33	52.3
July	27.2	11.4	1.7	0.21	25.6	13.4	1.5	0.24	1.0
August	27.1	9.9	1.7	0.18	25.3	11.8	1.4	0.19	1.3
September	24.0	7.2	1.3	0.18	22.4	9.5	1.2	0.18	14.2
2007	**Early Seral South**				**Old-Growth**				**CFH**
April	--	--	--	0.39	11.8	3.0	0.5	--	59.2
May	21.0	7.1	1.2	0.37	18.7	6.1	1.0	0.28	34.3
June	21.6	10.2	1.0	0.34	19.1	8.9	1.0	0.26	30.0
July	28.8	14.7	1.5	0.29	26.	13.5	1.5	0.23	18.8
August	25.1	12.1	1.3	0.26	22.8	11.0	1.2	0.20	15.5
September	23.0	9.5	--	0.27	19.0	8.4	0.9	0.18	57.7

2 Table 2.

3

4

5

6

7

8

9

10

11

12

13

14

15

1

Site	Upwind direction	Frequency	x_R (m), $_{R = 80\%}$	Available Fetch (m)	x_R: Instrument height	Available fetch: instrument height	Enough fetch
ESN06	0-45	2%	83.5	80	15:1	14:1	no
	45-90	6%	75.8	150	14:1	27:1	yes
	90-135	23%	78.8	80	14:1	14:1	no
	135-180	12%	78.0	130	14:1	24:1	yes
	180-225	15%	83.4	170	15:1	30:1	yes
	225-270	28%	95.8	210	17:1	38:1	yes
	270-315	11%	99.3	240	18:1	44:1	yes
	315-360	3%	92.5	90	17:1	16:1	no
		72%			**16:1**	**33:1**	**yes**
ESS07	0-45	4%	89.1	80	18:1	16:1	no
	45-90	29%	77.2	190	15:1	38:1	yes
	90-135	14%	83.0	200	17:1	40:1	yes
	135-180	5%	94.5	70	19:1	14:1	no
	180-225	13%	105.9	140	21:1	28:1	yes
	225-270	17%	105.3	160	21:1	32:1	yes
	270-315	14%	102.4	170	21:1	34:1	yes
	315-360	3%	114.2	50	23:1	10:1	no
		87%			**19:1**	**34:1**	**yes**

2 Table 3.

3

4

5

6

7

8

9

10

11

12

	ESN06			**OG06**			**ESS07**			**OG07**		
	May	July	Sept	May	July	Sept	May	July	Sept	May	July	Sept
R_n (W m^{-2})	384	553	410	620	661	518	487	463	345	666	698	506
G (W m^{-2})	NA	44.8	41.9	5.4	6.2	2.3	54.1	52.7	47.2	5.8	3.7	1.5
β	2.8 ± 1.1	0.78 ± 0.3	1.6 ± 0.8	2.2 ± 0.9	2.6 ± 1.0	1.9 ± 0.7	1.3 ± 0.6	0.94 ± 0.8	NA	2.6 ± 1.5	2.2 ± 1.4	2.0 ± 1.3
albedo	12-15%	12-15%	12-15%	7.2%	7.3%	7.9%	14.9%	13.7%	12.9%	7.9%	7.7%	8.4%

Table 4.

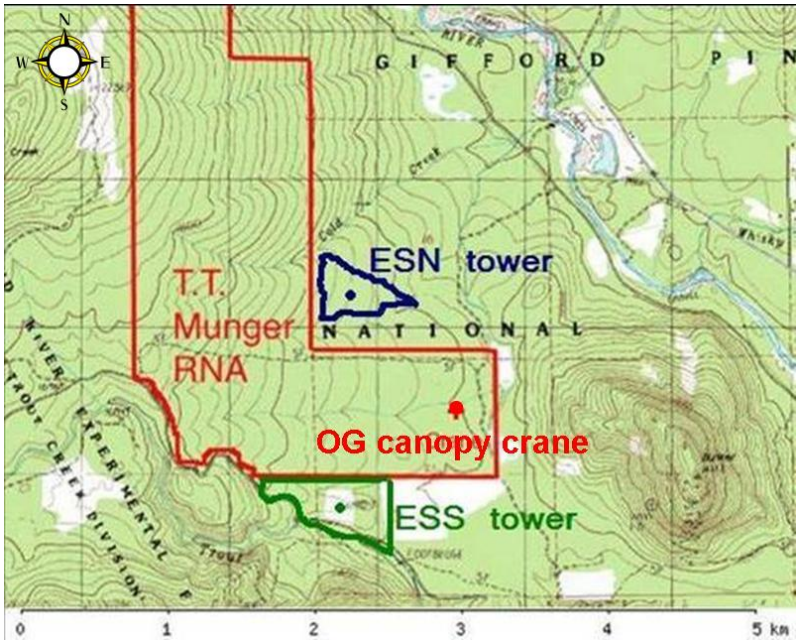
N
W
E
S
G I F F O R D
P I N
ESN tower
T.T.
Munger
RNA
N A T I O N A L
OG canopy crane
ESS tower
0
1
2
3
4
5 km

Fig 1.

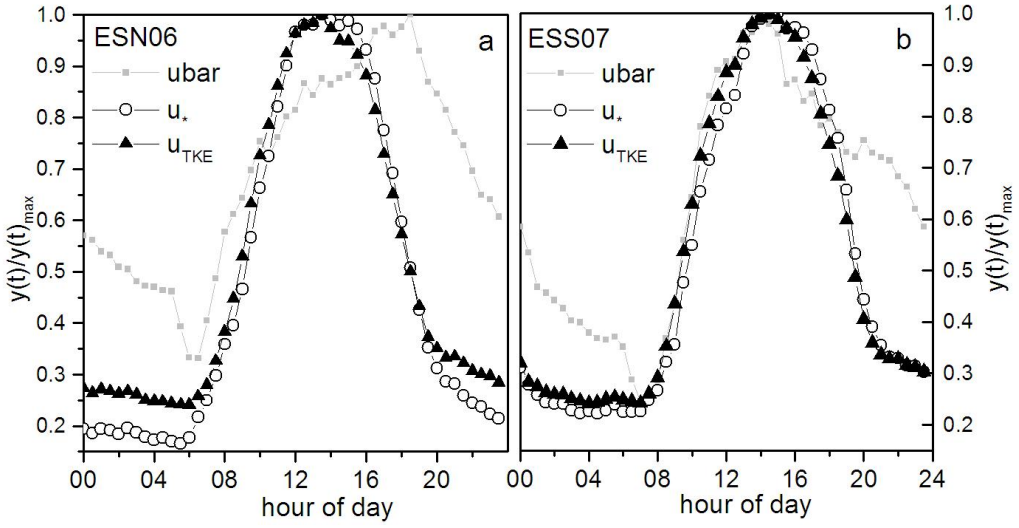
ESN06
a
ubar
u*
uTKE
ESS07
b
ubar
u*
uTKE
y(t)/y(t)max
hour of day
00
04
08
12
16
20
24
0.2
0.3
0.4
0.5
0.6
0.7
0.8
0.9
1.0

Fig 2.

1

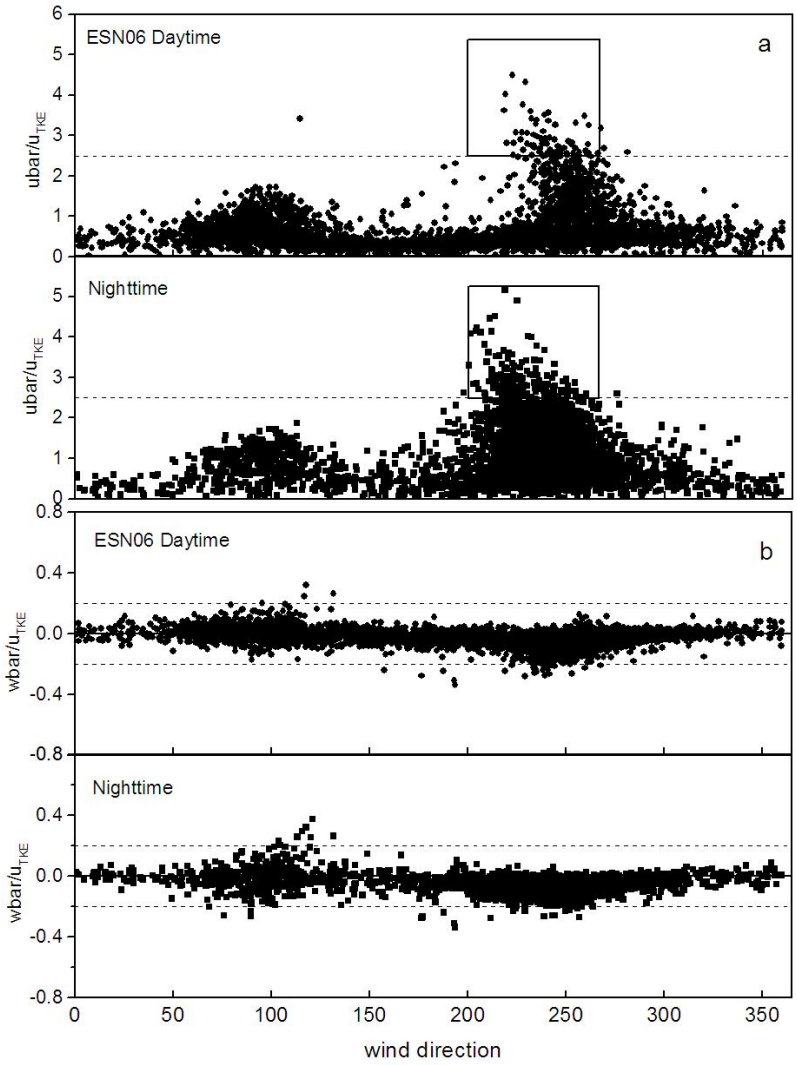

2

3 Fig 3.

4

5

6

7

8

9

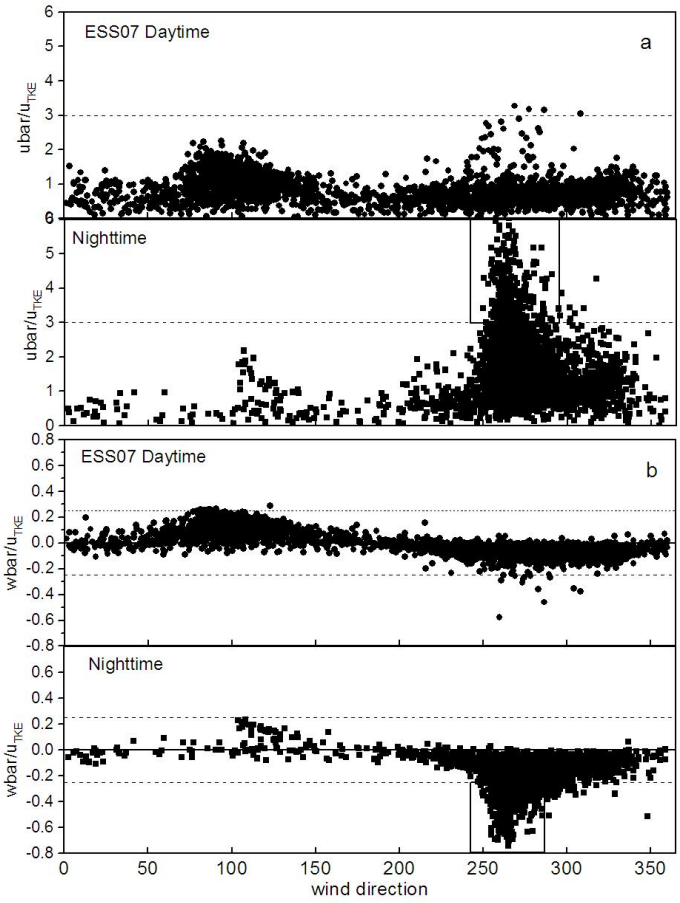
ESS07 Daytime
a
ubar/u*
Nighttime
ubar/u*
ESS07 Daytime
b
wbar/u*
Nighttime
wbar/u*
wind direction

Fig 4.

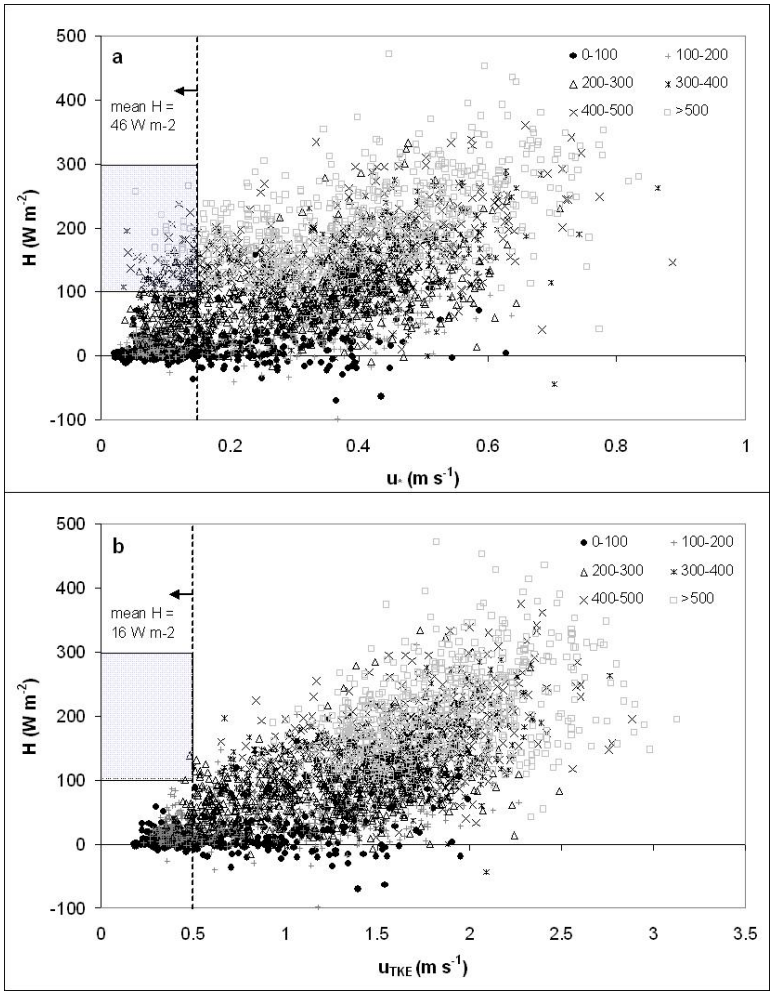
a
mean H =
46 W m-2
0-100
100-200
200-300
300-400
400-500
>500
H (W m-2)
u* (m s-1)
b
mean H =
16 W m-2
H (W m-2)
uTKE (m s-1)

Fig 5.

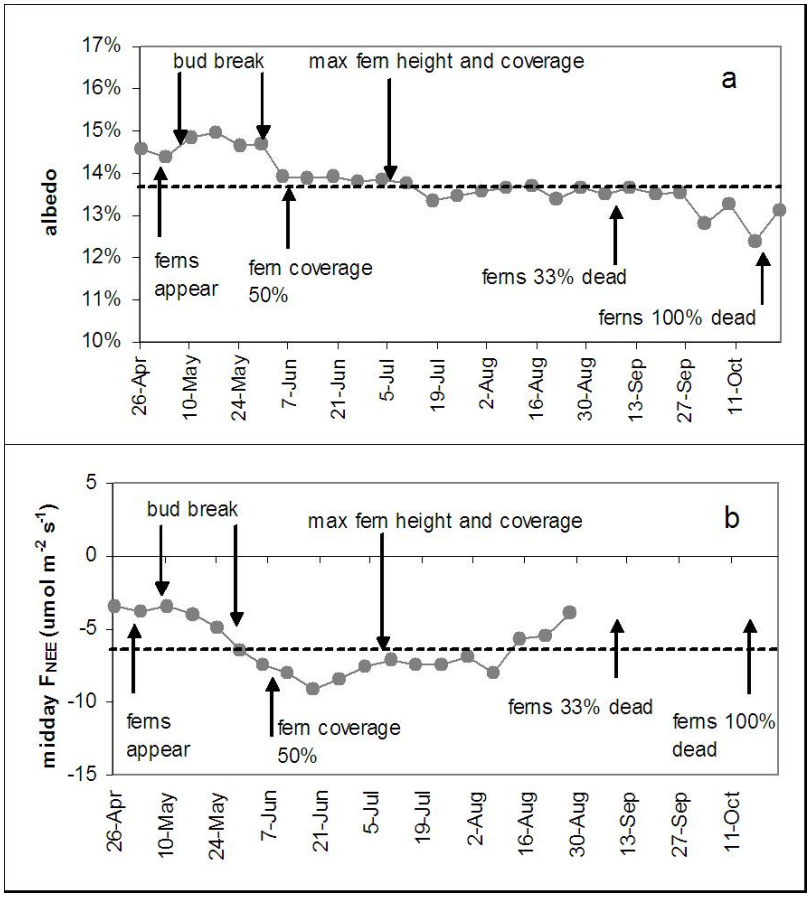
albedo
17%
16%
15%
14%
13%
12%
11%
10%
bud break
max fern height and coverage
a
ferns appear
fern coverage 50%
ferns 33% dead
ferns 100% dead
26-Apr
10-May
24-May
7-Jun
21-Jun
5-Jul
19-Jul
2-Aug
16-Aug
30-Aug
13-Sep
27-Sep
11-Oct
midday F_{NEE} (umol m^{-2} s^{-1})
5
0
-5
-10
-15
bud break
max fern height and coverage
b
ferns appear
fern coverage 50%
ferns 33% dead
ferns 100% dead
26-Apr
10-May
24-May
7-Jun
21-Jun
5-Jul
19-Jul
2-Aug
16-Aug
30-Aug
13-Sep
27-Sep
11-Oct

Fig 6.

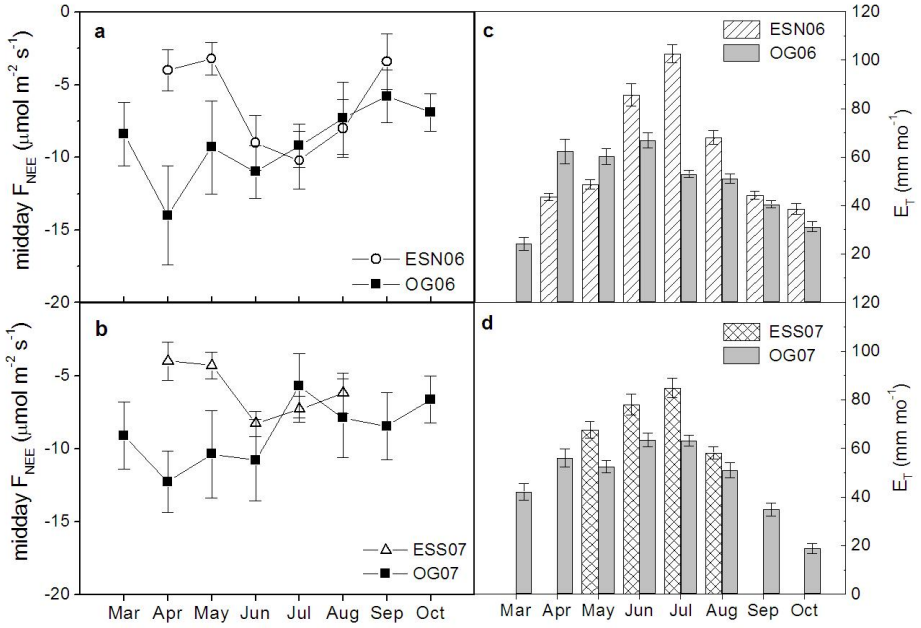
a
b
c
d
midday F_{NEE} (μmol m^{-2} s^{-1})
E_T (mm mo^{-1})
ESN06
OG06
ESS07
OG07
Mar Apr May Jun Jul Aug Sep Oct

Fig 7.

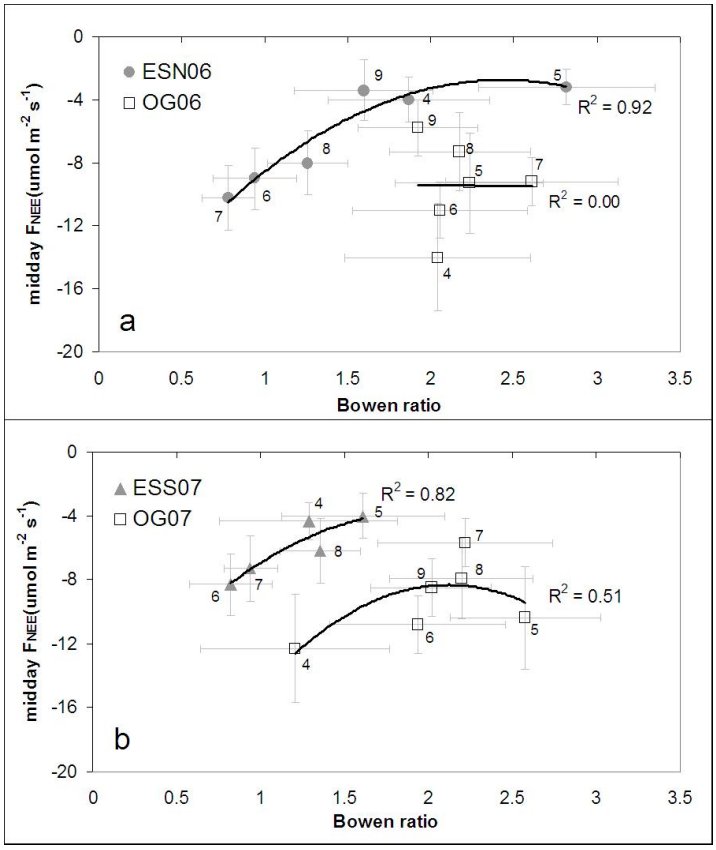
ESN06
OG06
R^2 = 0.92
R^2 = 0.00
a
midday F_{NEE}(umol m^{-2} s^{-1})
Bowen ratio
ESS07
OG07
R^2 = 0.82
R^2 = 0.51
b
midday F_{NEE}(umol m^{-2} s^{-1})
Bowen ratio

Fig 8.

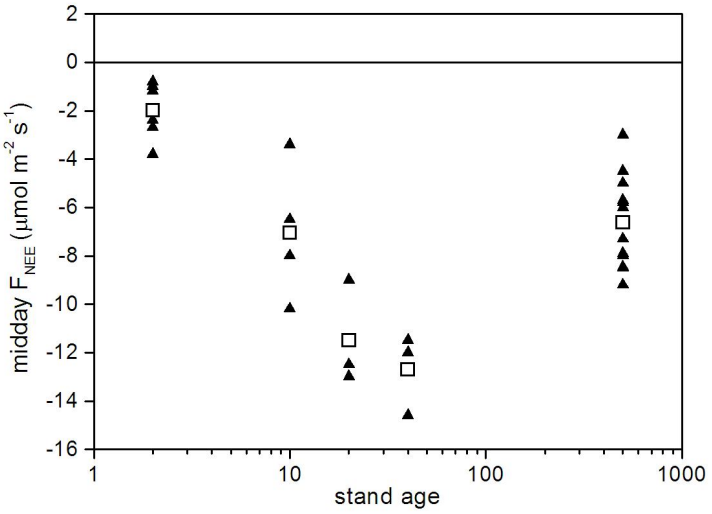
2
0
-2
-4
-6
-8
-10
-12
-14
-16
midday F_{NEE} (µmol m^{-2} s^{-1})
1
10
100
1000
stand age

Fig 9.